Indonesian Geotechnical Journal, April 2023, Vol 2 (1). Page 53 - 65
DOI: https://doi.org/10.56144/igj.v2i1.21
E-ISSN:2829-7520
https://indonesian-geotechnical-journal.org/index.php/IGJ/issue/archive

Study of Strain-rate Effect in Two-dimensional Biaxial Test on Granular Material using Discrete Element Method

Ananda Putri Swastinitya[1], Jessica Sjah[2,*], James Jatmiko Oetomo[3]
[1]Civil Engineering, Faculty of Engineering, Universitas Indonesia, Depok, Indonesia, 16424; ananda.putri12@ui.ac.id
[2]Civil Engineering, Faculty of Engineering, Universitas Indonesia, Depok, Indonesia, 16424; jessicasjah@eng.ui.ac.id
[3]PT Geostruktur Sistem Solusindo, Jakarta, Indonesia, 11750; james@geostruktur.com
*Correspondence: jessicasjah.ui@gmail.com

SUBMITTED 23 November 2022 **REVISED** 13 March 2023 **ACCEPTED** 17 March 2023

ABSTRACT Numerical study to investigate the effect of various strain rates on global friction angle in sand has been performed. Granular material behavior is influenced by several factors, among others: pack configuration, grain macro and micro roughness, confinement pressure, loading rate, etc. Sand is a granular material composed of discrete particles that require refined microscopic techniques to study its mechanical properties. The two-dimensional Discrete Element Method (DEM) is capable of calculating the motion and interparticle contacts of large number of particles, where each particle is modeled as a rigid circular element. In Indonesia, research related to the DEM is still very limited. The study is commenced with the validation of DEM model using YADE. Particles with a local friction angle of 35° were arranged in a closed rectangular box (frictionless wall). The number of particles used in this validation simulation model are 1000 sphere-type particles with monodisperse particle gradations. The simulation was done by a drained biaxial test with confinement stress of 100 kPa, thereafter varying strain rates were applied. Based on the deviatoric stress–axial strain curve from YADE, results can be depicted with Mohr circles for obtaining the global friction angle. It was found that different value of strain rates affects the global friction angle. In this study, increasing the strain rate from 1% s^{-1} to 5% s^{-1}, 10% s^{-1}, 25% s^{-1}, and 50% s^{-1} will increase its global friction angle by 5%, 5%, 14%, and 18%, respectively.

KEYWORDS Granular material, Discrete Element Method, strain rate, local-global friction angle, drained biaxial test

1 INTRODUCTION

Granular material is a material composed of a collection of particles and is commonly found in nature. Its behavior is influenced by several factors, among others: pack configuration, grain macro and micro roughness, confinement pressure, loading rate, etc. Soil shear strength describes the strength of soil to carry loads, beyond which a collapse (e.g., landslides) may occur. The stress-strain or force-displacement of material is governed by a certain constitutive law which can be implemented in macro or micro level, depending on the model being used. The typical industry approach is by using a finite element model; however, in the case where a large deformation or a very localized displacement occurs, a discrete element model is more powerful at understanding the micro-mechanical behavior of sand. Due to considerable changes in the mechanical properties of microstructure during shearing, performing particulate-scale analysis is advantageous; however usually smaller specimen size is adopted for limiting the computational cost (Huang et al., 2008).

The triaxial test is the most common method for determining soil mechanics properties. The first loading phase in a triaxial test is a confinement phase where compressive pressure is applied on the specimen, after that a deviatoric stress is applied to the specimen. Confinement stress is used to simulate the in-situ compression pressure of the specimen, while deviatoric stress aims to apply incremental shear load up to failure so that the soil shear strength is known. The strain rate in the triaxial test affects the resulting soil shear strength. Thus, it is interesting to see the influence of this strain rate at the particulate scale using Discrete Element Method (DEM).

An experimental test conducted by Lee et al. (1969) aimed to investigate the effect of strain rate on dry and saturated sand in loose and dense packing under a consolidated drained triaxial test; their results showed that an increase in strain rate produced an increase in strength. Yamamuro et al. (2011) performed an experimental test on crushed coral sand under the different values of strain rates varied from approximately 0.0022 to 1750% s^{-1}; they showed that increasing strain rate will increase shear strength moderately. Das et al. (2022) studied the effects of strain rate on the critical state response of crushable sand subjected to a drained triaxial test simulated using DEM under different initial confining pressures and initial densities; they showed that a higher strain rate produces higher strength in terms of both peak stress and residual stress. Indeed, these studies showed that strain rate can affect the mechanical response of material.

The Discrete Element Method (DEM) was first proposed by Cundall and Strack in 1979. Conceptually, DEM is the most physically representative numerical method for simulating granular materials. DEM simulate the micromechanical response by considering the shapes, movement, and contact forces on each particle at the micro-scale. The mechanical response of the granular material in DEM is controlled by contacts between adjacent particles and contacts between particles and domain walls (boundaries). Consequently, the physical quantities that control this interaction such as particle rotation, particle orientation, contact forces, and so on can be calculated easily, which is very difficult to obtain in experimental tests. Two important components in DEM are the particles and the interactions between particles. Particles can have different shapes, sizes, and distributions within a single domain. In this study, the shape of the particle is taken as a soft-sphere (circle in 2D). There are two types of particle spheres in DEM: soft-sphere and hard-sphere. In soft-sphere type, particles are rigid but overlaps between the particles are allowed; it allows simultaneous contacts between particles. In contrast, contacts in hard-sphere type are not simultaneous where there is only one collision contact at a time.

During the DEM simulation, particle interactions (i.e., contact) can be formed dynamically and it may break during the analysis process. This interaction between particles occurs when the distance between the two particles is zero. When the distance between the two particles is negative, there is an overlap, hence a compressive force occurs between the particles. According to Tannu (2017), four main things that need to be considered in the DEM modeling are: particle generation and distribution, initialization of bonds, contact model, and bond failure. The initialization stage includes the process of arranging the numerical sample (particle generation and distribution), followed by the bond initialization phase (if used). Once the numerical specimen has been generated (with a contact model of choice), then loading sequences can be started.

In Indonesia, research related to the Discrete Element Method is still very limited. DEM can analyze micromechanics process in detail. Moreover, it can also produce quite accurate results in modeling granular or discontinuous materials when experimental tests are difficult or cost prohibitive. In this paper, the strain rate effect as contributed from the inertial effect of dynamic system is studied. As an initial part of research related to DEM in Indonesia, the two-dimensional (2D) Discrete Element Method is used.

2 METHODS

2.1 Model Validation

To ensure that the discrete element model represent the actual specimen, a validation model was carried out based on a numerical study conducted by Nguyen et al. (2016). In the research by Nguyen et al. (2016) the numerical model validation phase was carried out on the 3D DE model and then compared with the results of an experimental study conducted by Royis & Doanh (1998) and numerical study conducted by Calvetti et. al. (2003). Then, Nguyen et al. (2016) switches to 2D DE modeling using YADE, citing easier particle visualization and faster computational time. Because the current study also uses a 2D DE model using YADE, the model validation stage in this study will only refer to the 2D DEM results from Nguyen et. al. (2016).

In the study conducted by Nguyen et al. (2016), a static biaxial drained test is conducted on 20000 particles generated randomly inside a rectangular box domain sized 0.198×0.198 meters. There is no friction on the domain wall (frictionless wall). The strain rate value used in the simulation is 1%/s. Due to the limited information related to the material size gradation inside the domain and for reducing the simulation time so that the simulation is not too time-consuming, the number of particles used in the model validation simulation is set to 1000 sphere-type particles with monodisperse particle gradation. The grain density used in the simulation is 3000 kg/m^3, which is also referred from Nguyen et al. (2016).

To prepare the packing, 1000 spheres are randomly generated inside the domain box with constructive algorithm particle generation and distribution method. Based on Gyurko et al. (2014), the constructive algorithm method is considered the most efficient because in this method the particles will be formed in a closed domain and they are not distributed dynamically. More precisely, particles with a certain radius are placed at random positions in the desired domain, without overlapping. If overlap occurs, the newly created particle will be removed from the model. This process is repeated until the domain box is filled. As these particles are randomly generated, even with identical input parameters, particle generation carried out at different times can have different initial particle position (and slightly different two-dimensional porosity), hence producing different results. For maintaining the initial pack configuration, this can be done by exporting data in the form of x, y, and z coordinates and the radius of each particle. Thus, the position of particles will remain the same for every simulation, as well as its two-dimensional initial porosity.

Once particles have been generated, the packing is compressed by applying an isotropic stress on the wall as confinement stress, in this case $\sigma_1' = \sigma_2' = 100\text{kPa}$. The biaxial drained test is continued by applying a strain rate $\epsilon_2 = 0.01\text{s}^{-1}$, while the lateral stress is kept constant at $\sigma_1' = 100\text{kPa}$. To simulate the biaxial-drained test on YADE, there are several simulation engine that can be used. The simulation engine used in this study is TriaxialCompressionEngine. The Linear Elastic-Plastic type contact model as proposed by Cundall (1979) has been used.

The Linear Elastic-Plastic contact model is the primary type of contact model in the DEM modeling (see Figure 1). In this contact model, the normal force (F_n) is a linear function of normal displacement, while shear force (F_s) is a linear function of shear or tangential displacement. In principle, the calculation is carried out by applying Newton's 2nd law and the micro-mechanic contact law in iterative manner. Newton's 2nd law calculates the motion of the particle due to the force acting on the particle, while the micro-mechanic contact law is implemented to calculate the magnitude of the contact force due to displacement.

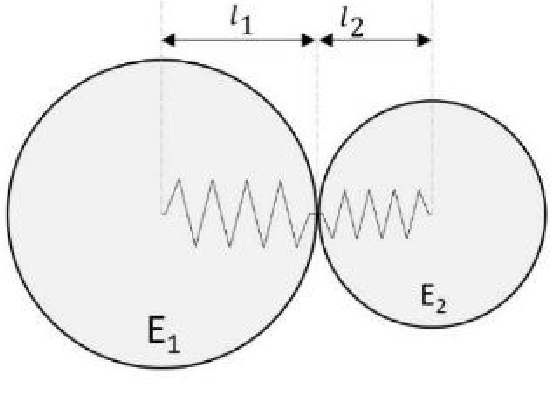

Figure 1. Normal stiffness in the contact area between particles in the Linear Elastic-Plastic contact model.

For the DEM modeling in this study, YADE was used. It is an open-source software based on the discrete element method (DEM) which uses object-oriented programming techniques with the programming language Phyton. For the DEM modeling, YADE uses a time-integration scheme (Lagrangian method) to determine the position, orientation, velocity, and angular velocity of the simulated particles. The forces and moments acting on each particle are stored at each time step. The contact force depends on the overlap of the particles and their material properties.

In YADE, particles in contact are connected by imaginary springs in the local principal directions which describes the normal k_n and tangential stiffness k_s of contacts. The normal stiffness k_n is directly related to the elastic modulus of each particle where the total length of the normal spring is the sum of spring length of each particle (l_1 and l_2, see Figure 1). The normal stiffness k_n is formulated with Eq. (1), where E is modulus elasticity of particles and A is contact area between two particles (determined with Eq. (2)). The tangential stiffness k_s is calculated with Eq. (3), where v is the local Poisson ratio.

$$k_n = \left(\frac{l_1}{E_1 A} + \frac{l_2}{E_2 A}\right)^{-1} \tag{1}$$

$$A = \pi \min(l_1, l_2)^2 \tag{2}$$

$$k_s = v k_n \tag{3}$$

According to Sibille (2006), an interparticle friction angle ϕ of 35° makes it possible to simulate reasonable mechanical responses despite the particle spherical shape. It should be noted that the particles formed in YADE are spherical (3D), but to form two-dimensional models (disks), spheres can be set as disks by blocking the movement and rotation of particle in the third plane (3-direction in Figure 2 and Figure 3). Also, it must be noted that, in this study, simulations are carried out without gravity. Typical model parameters are shown in Table 1.

Table 1. Model parameters

Parameter	Value
Density of particles	3000 kg/m^3
k_n/D_{sphere}	5×10^9 Pa
v	0.42
ϕ_{sphere}	35°
Wall friction	0°
2D void ratio at isotropic state	0.221
2D porosity at isotropic state	0.181 (dense)

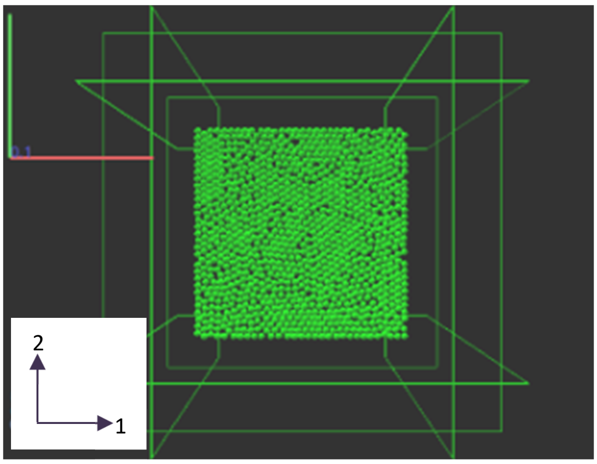

Figure 2. Particle pack using DEM in YADE (1-2 plane)

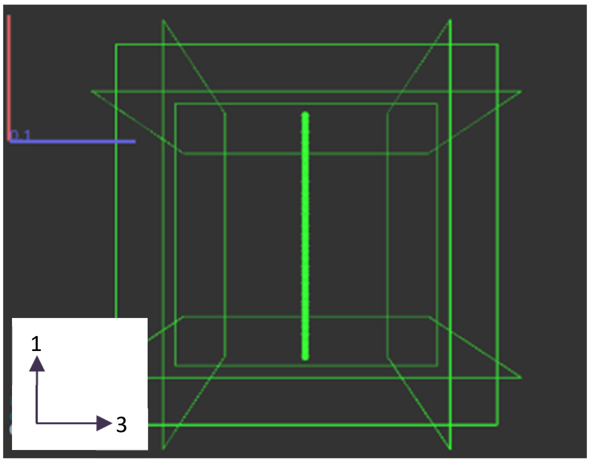

Figure 3. Particle pack using DEM in YADE (3-1 plane).

The validation process for the YADE model is carried out by comparing the axial strain-deviatoric stress curve from previous studies and the simulation results carried out by the author. Results can be depicted with Mohr circles for obtaining the global friction angle, wherein σ'_1 is the major principal effective stress, σ'_2 is the value of confinement stress, and ϕ' is the global friction angle. Based on the applied/measured global stress (see Figure 4), the friction angle can be calculated using Eq. (4).

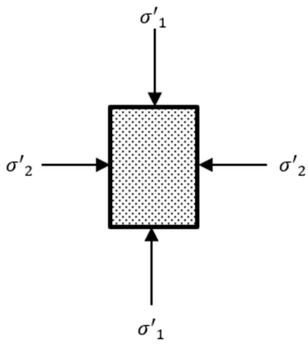

Figure 4. Principal global stress in the numerical specimen.

$$\sigma'_1 = \sigma'_2 tan^2\left(45 + \frac{\phi'}{2}\right) + 2c'tan\left(45 + \frac{\phi'}{2}\right) \quad (4)$$

2.2 Parametric Study

Current study aims to investigate the effect of various strain rates on global friction angle of sand. In this study, the independent variable is the strain rate. The controlled variables are the domain size of 0.198×0.198 meters; contact model is Linear Elastic-Plastic type, with material properties as tabulated in Table 1. The dependent variables are the sand micro-macro mechanics properties due to the drained biaxial test and the strain rate variations as shown in Table 2.

Table 2. Global friction angle parametric study results.

Strain rate (s^{-1})	Simulation Code
0.1%	SR0_1
0.5%	SR0_5
1%	SR1
5%	SR5
10%	SR10
25%	SR25
50%	SR50

3 RESULTS

3.1 DE Model Validation Results

Figure 5 shows the deviatoric stress – axial strain results from our YADE DEM model compared with results from Nguyen et al. (2016). The delay in peak stress is caused by physical movement during the shearing process (rolling and sliding); this is the advantage of DEM approach where one may observe the micromechanical processes during the shearing. This physical evolution depends primarily on the particle contact law, initial packing density/porosity, particle shape, and confinement stress. The corresponding volumetric strain/void ratio in function of axial strain is shown in Figure 6.

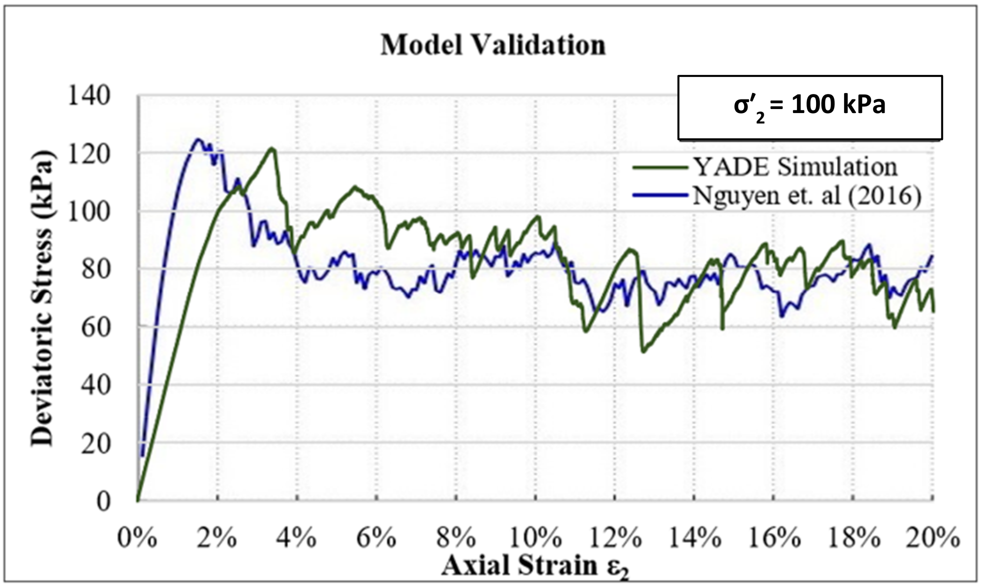

Figure 5. Deviatoric stress–axial strain from YADE simulation with strain rate value of 1% s^{-1}: (green) this study; (blue) Nguyen et al. (2016).

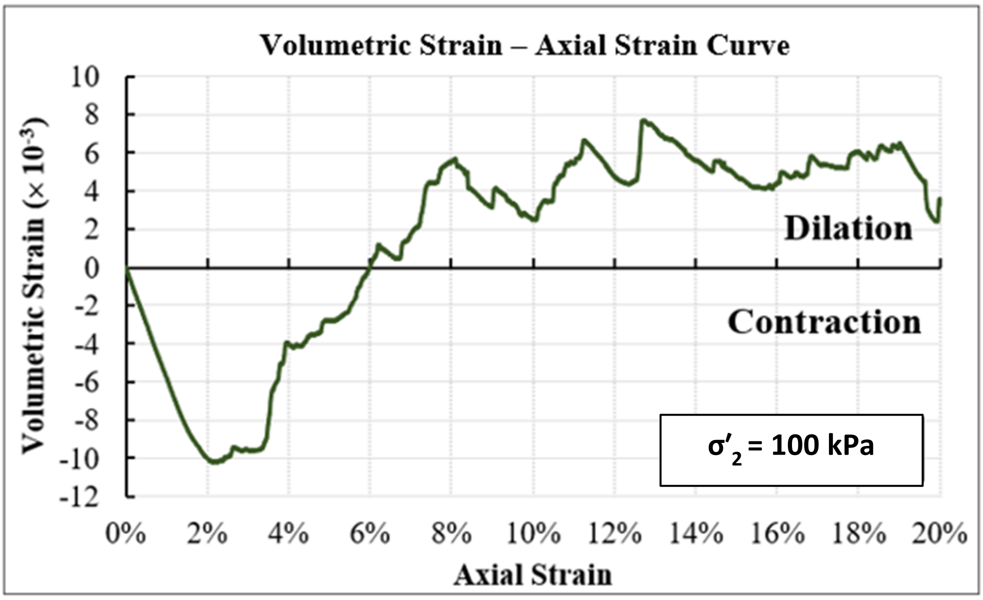

Figure 6a. Volumetric strain – axial strain from YADE simulation with strain rate value of 1% s^{-1}.

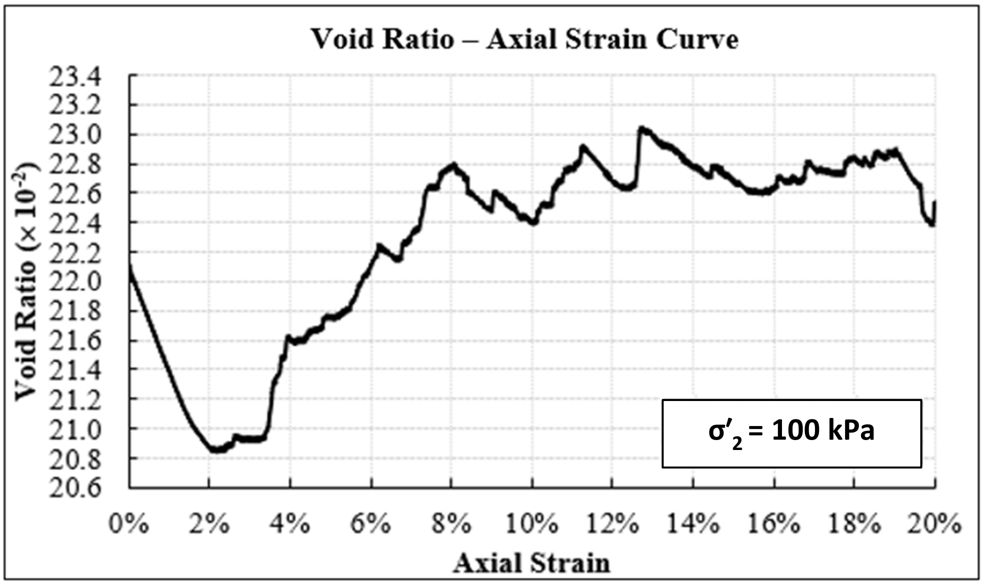

Figure 6b. Two-dimensional (2D) void ratio – axial strain from YADE simulation with strain rate value of 1% s^{-1}.

3.2 Parametric Results

Figure 7 shows the deviatoric stress – axial strain curve with various strain rate values as described in Table 2; the corresponding volumetric strain evolution can be seen in Figure 8. From these results, corresponding peak deviatoric stresses have been tabulated in Table 3. We can remark that the application of higher strain rate will yield higher strength.

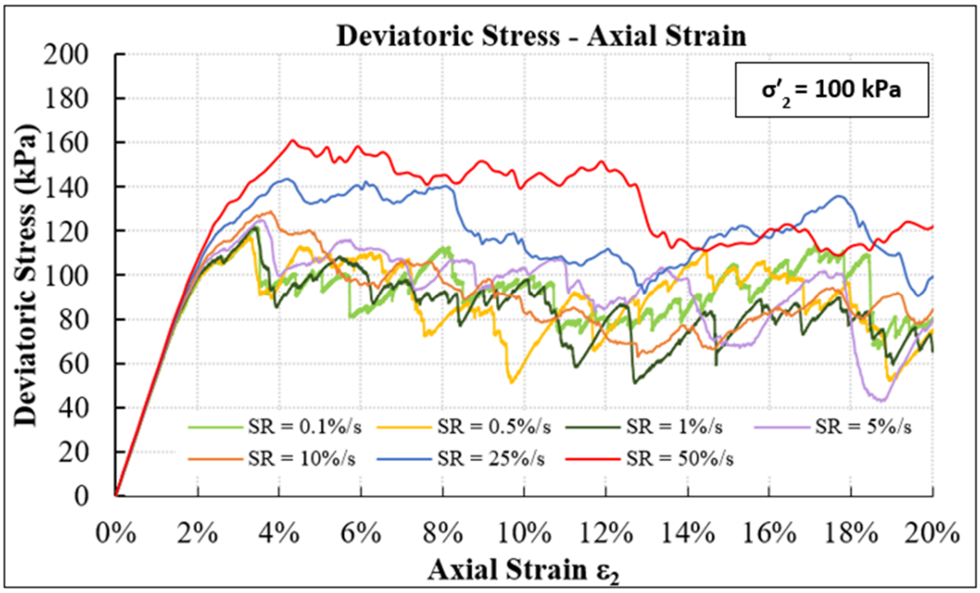

Figure 7. Deviatoric stress – axial strain curve parametric study results.

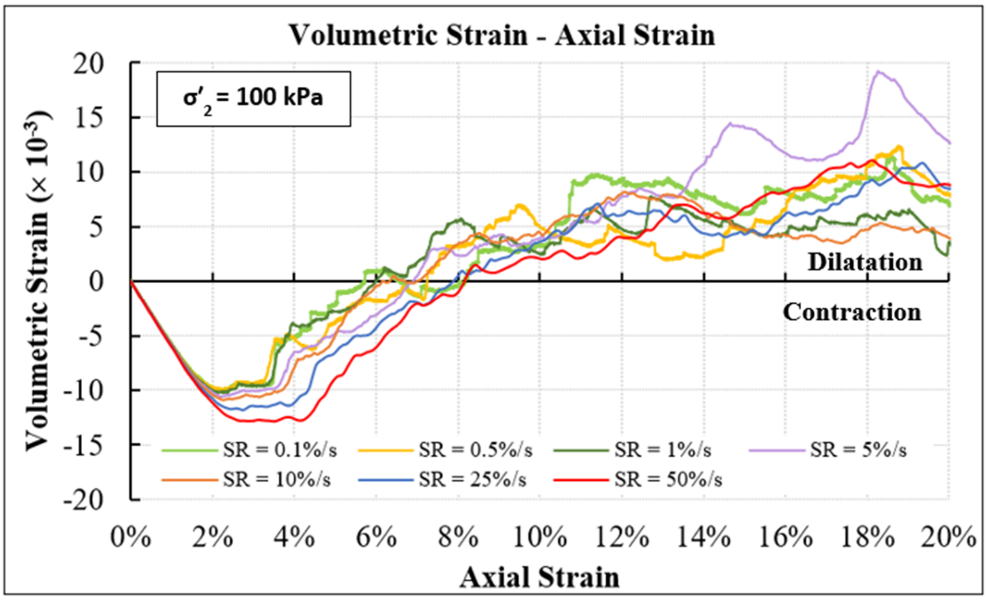

Figure 8. Volumetric strain – axial strain curve parametric study results.

Table 3. Global friction angle parametric study results.

Simulation Code	Strain rate (s^{-1})	Peak Deviatoric Stress (kPa)	Global Friction Angle (°)
Nguyen et al. (2016)			
	1%	125	23
Parametric Study			
SR0_1	0.1%	121.476	22
SR0_5	0.5%	116.859	22
SR1	1%	121.390	22
SR5	5%	124.928	23
SR10	10%	128.730	23
SR25	25%	143.486	25
SR50	50%	160.995	26

4 DISCUSSION

From the drained biaxial test, the global stresses and strains acting on each plane (1, 2, and 3-plane), as well as the three-dimensional porosity of the packing, can be measured. The deviatoric stress is calculated by subtracting σ_1' with the confinement stress (100 kPa). The volumetric strain of the two-dimensional model is calculated by summing strains from the two principal directions. However, it must be noted that the porosity of the packing in the biaxial test is two-dimensional porosity.

As observed in Figure 5 there is a slight difference between the deviatoric stress–axial strain curve between Nguyen et al. (2016) results and current study, especially during the elastic phase. It is caused due to a difference in the two-dimensional DE model initial porosity. The initial porosity of Nguyen et al. (2016) is 0.167 (2D void ratio of 0.201) while the initial porosity of DE model conducted by the author is 0.181 (2D void ratio of 0.221). Hence, the difference in two-dimensional initial porosity is about 8%. Nonetheless, the peak and residual strength results on both studies are similar.

Figure 6a shows the axial strain – volumetric strain results on a two-dimensional DE model tested with strain rate of 1% s^{-1}. It shows that the volumetric response of the material at the initial part of elastic stage undergoes contraction, and as the material enters an inelastic stage the volumetric response tends to dilate. This behavior is in accords with the expected dense soil packing behavior.

In the study by Nguyen et al. (2016), the deviatoric stress reached a peak of 125 kPa at an axial strain of 1.5%, whereas on the model validation simulation, the deviatoric stress reaches a peak of 121.390 kPa at an axial strain of 3.36%. Afterward, a strain-softening phase is observed and the curve tends to plateau until the end of the simulation. The peak deviatoric stress difference between Nguyen et al. (2016) and current study is about 2.8%. Furthermore, with a particle (i.e., local) friction angle of 35°, using equation (4), the global friction angle in Nguyen et al. (2016) study is 23°; whilst, our study yields a global friction angle of 22°. Therefore, considering a close agreement between the two, our 2D DEM model is considered valid and it will be used for the parametric study.

Various strain rate values have been tested to the two-dimensional discrete element sand model using YADE. As seen in Figure 7, strain rate values have an influence on the deviatoric stress – axial strain curve results. Results of the parametric study (see Table 3) show that the greater the strain rate value, the greater the deviatoric stress that occurs, therefore the greater the global friction angle. In this case, if the given strain rate value is less than or equal to 1% s^{-1}, the global friction angle of the sand shows the same value, which is 22°.

When the applied strain rate exceeds 1% s^{-1}, the global friction angle increases. Increasing the strain rate value from 1% s^{-1} to 5% s^{-1} and 10% s^{-1} will increase the global friction angle by about 5%. By increasing in the strain rate value from 1% s^{-1} to 25% s^{-1} and 50% s^{-1}, the global friction angle increases by 14% and 18%, respectively. This shows that the global friction angle will increase significantly if the strain rate value applied to the two-dimensional DEM simulation exceeds 1% s^{-1}. It should also be highlighted that, in current study, the strain rate effect can be attributed to the inertial effect in DEM simulation. The inertial effect is controlled by local damping parameter which is set to 0.9 in this study.

On the other hand, using strain rate values of 0.1% s^{-1}, 0.5% s^{-1}, and 1% s^{-1}, the differences in the value of the deviatoric stress and the global friction angle are not significant, indicating a quasi-static condition. Considering that the deviatoric stress – axial strain evolution for these cases are very closes one-to-another, especially up to axial strain of around 4%, the drop of peak deviatoric stress in SR0_5 (compared to SR0_1) can be attributed to the inherent statistical variation of the peak deviatoric stress, as each simulation still undergo a slightly different plastic evolution.

5 CONCLUSION

The effect of strain rate on granular material (sand) subjected to drained-biaxial test, using the discrete element method (DEM), has been carried out using YADE software.

A validation model was performed to ensure a reliable two-dimensional DE model. The two-dimensional DE model has a close agreement with a reference study from Nguyen et al. (2016), with a relative error of 4% (in terms of global friction angle). This difference could be attributed to the limited information regarding particle gradation in the reference study, as well as a difference in the two-dimensional initial porosity. The two-dimensional initial porosity on the reference paper is 0.167 (2D void ratio of 0.201), while on the DE model generated by the author, it is 0.181 (2D void ratio of 0.221). With a relative error of less than 10% (in terms of peak deviatoric stress), the DE model can be used for parametric studies.

Furthermore, based on the axial strain - volumetric strain curve, the volumetric response at the initial part of elastic stage undergoes contraction; further on, when it enters an inelastic stage, the volumetric response tends to dilate. This behavior corresponds well to the dense soil packing behavior, an expected result.

Based on results of parametric studies, the greater the strain rate value, the greater the deviatoric stress that occurs. Thus, the global friction angle increases in function of increasing strain rate. However, with a strain rate of 0.1% s^{-1}, 0.5% s^{-1}, and 1% s^{-1} the global friction angle value will not increase significantly (if any). Meanwhile, by increasing strain rate values from 1% s^{-1} to 5% s^{-1}, 10% s^{-1}, 25% s^{-1}, and 50% s^{-1} the global friction angle value will increase by 5%, 5%, 14%, and 18%, respectively.

Thus, we can highlight the following: (1) using a strain rate of approximately 1% s^{-1} will yield a quasi-static result and (2) applying larger strain rate than 1% s^{-1} will essentially increase the peak deviatoric stress/global friction angle. This shows the DEM capability to simulate the strain rate effect where this dynamic effect can be considered even with a standard (Linear Elastic-Plastic) contact model.

DISCLAIMER

All authors declare that we have no conflicts of interest. The funders had no role in the design of the study, in the collection, analysis, or interpretation of data, in the writing of the manuscript, or in the decision to publish the results.

AVAILABILITY OF DATA AND MATERIALS

The authors confirm that the data supporting the findings of this study are available within the article and/or its supplementary materials. The derived data presented in this study are available on request from the corresponding author. The derived data are not publicly available due to privacy restrictions.

ACKNOWLEDGMENTS

This research is supported by Lembaga Pengelola Dana Pendidikan (LPDP) or the Indonesia Endowment Fund for the Education Republic of Indonesia.

REFERENCES

ASTM D7181-20., 2020. *Standard test method for consolidated drained triaxial compression test for soils*. ASTM International. https://doi.org/10.1520/D7181-20.of

Bakunowicz, P., 2014. *Discrete element modelling of CPT using shaking table tests in sands*. Izmir Institute of Technology (Turkey). Burman, B. C., Cundall, P. A., Strack, O. D. L., 1980. A discrete numerical model for granular assemblies. *Géotechnique*, 30(3), pp. 331–336. https://doi.org/10.1680/geot.1980.30.3.331

Chen, C., Gu, J., Peng, Z., Dai, X., Liu, Q. & Zhu, G. Q., 2022. Discrete element modeling of particles sphericity effect on sand direct shear performance. *Scientific Reports,* 12(1), pp. 1–14. https://doi.org/10.1038/s41598-022-09543-9

Chen, Q. et al., 2019. Effect of fine-grained dipping interlayers on mechanical behavior of tailings using discrete element method. *Engineering Analysis with Boundary Elements,* 104, pp. 288–299. https://doi.org/10.1016/j.enganabound.2019.03.029

Cheung, G. & O'Sullivan, C., 2008. Effective simulation of flexible lateral boundaries in two- and three-dimensional DEM simulations. *Particuology*, 6(6), pp. 483–500. https://doi.org/10.1016/j.partic.2008.07.018

Duriez, J., Scholtès, L. & Donzé, F. V., 2016. Micromechanics of wing crack propagation for different flaw properties. *Engineering Fracture Mechanics*, 153, pp. 378–398. https://doi.org/10.1016/j.engfracmech.2015.12.034

EN ISO 14688-1., 2018. *Geotechnical investigation and testing, Identification and classification of soil, Part 1: Identification and description*. British Standards Institution.

Fu, R., Hu, X. & Zhou, B., 2017. Discrete element modeling of crushable sands considering realistic particle shape effect. *Computers and Geotechnics*, 91, pp. 179–191. https://doi.org/10.1016/j.compgeo.2017.07.016

Grabowski, A., Nitka, M. & Tejchman, J., 2021. 3D DEM simulations of monotonic interface behaviour between cohesionless sand and rigid wall of different roughness. *Acta Geotechnica*, 16(4), pp. 1001–1026. https://doi.org/10.1007/s11440-020-01085-6

Gyurkó, Z., Bagi, K. & Borosnyói, A., 2014. Discrete Element Modelling of uniaxial compression test of hardened concrete. *Építöanyag - Journal of Silicate Based and Composite Materials*, 66(4), pp. 113–119. https://doi.org/10.14382/epitoanyag-jsbcm.2014.21

Hosseininia, E. S., 2012. Investigating the micromechanical evolutions within inherently anisotropic granular materials using discrete element method. *Granular Matter*, 14(4), pp. 483–503. https://doi.org/10.1007/s10035-012-0340-5

Huang, Z. Y., Yang, Z. X. & Wang, Z. Y., 2008. Discrete element modeling of sand behavior in a biaxial shear test. *Journal of Zhejiang University-Science A,* 9(9), pp. 1176–1183. https://doi.org/10.1631/jzus.A0720059

Ishihara, K., Tatsuoka, F., & Yasuda, S., 1975. Undrained deformation and liquefaction of sand under cyclic stresses. *Japanese Society of Soil Mechanics and Foundation Engineering*, 15(1), pp. 29–44.

Jiang, M. and Yu, H.S., 2006. *Application of discrete element method to geomechanics* (pp. 241-269). Springer Berlin Heidelberg.

Joshi, A. N., 2018. *A Discrete Element Study of the Uniaxial Compressive*. United States: Master Thesis Report, Department of Mechanical Engineering, The University of North Carolina at Charlotte.

Kafashan, J., Wiącek, J., Abd Rahman, N. & Gan, J., 2019. Two-dimensional particle shapes modelling for DEM simulations in engineering: a review. *Granular Matter*, 21(3). https://doi.org/10.1007/s10035-019-0935-1

Kozicki, J. & Donze, F. V., 2009. YADE-OPEN DEM: An opensource software using a discrete element method to simulate granular material. *Engineering Computations*, 26(7), pp. 786–805. https://doi.org/10.1108/02644400910985170

Kozicki, J. & Tejchman, J., 2011. Numerical simulations of sand behaviour using dem with two different descriptions of grain roughness. *Proceedings of Particle-Based Methods II - Fundamentals and Applications*, pp. 62–71.

Lambe, T. W. & Whitman, R. V., 1969. *Soil Mechanics.* New York: John Wiley & Sons.

Li, Z., 2017. *Validations and Applications of Discrete Element Method*, Hong Kong: Doctoral Thesis Report. Department of Civil and Environmental Engineering. The Hong Kong University of Science and Technology.

Luding, S., 2008. Introduction to discrete element methods: Basic of contact force models and how to perform the micro-macro transition to continuum theory. *European Journal of Environmental and Civil Engineering,* 12(7–8), pp. 785–826. https://doi.org/10.1080/19648189.2008.9693050

Matuttis, H. & Chen, J., 2014. *Understanding the Discrete Element Method.* Singapore: John Wiley & Sons.

Markauskas, D. & Kačianauskas, R., 2006. Compacting of particles for biaxial compression test by the discrete element method. *Journal of Civil Engineering and Management*, 12(2), pp. 153–161. https://doi.org/10.1080/13923730.2006.9636387

Nguyen, H., 2016. *The role of the microstructure in granular material instability,* France: Doctoral Thesis Report. Department of Civil Engineering. Université de Lyon.

Popp, A. & Wriggers, P., 2018. Contact Modeling for Solids and Particles. *In Contact Modeling for Solids and Particles* (Vol. 585). Springer International Publishing. https://doi.org/10.1007/978-3-319-90155-8

Potyondy, D. O. & Cundall, P. A., 2004. A bonded-particle model for rock. *International Journal of Rock Mechanics and Mining Sciences,* 41(8), pp. 1329–1364. https://doi.org/10.1016/j.ijrmms.2004.09.011

Qu, T., Feng, Y. T., Wang, Y. & Wang, M., 2019. Discrete element modelling of flexible membrane boundaries for triaxial tests. *Computers and Geotechnics,* 115. https://doi.org/10.1016/j.compgeo.2019.103154

S.K. Das, S.K. Verma, and A. Das, 2022. Numerical assessment of effects of strain rate on the critical state of crushable sand. *Géotechnique Letters*, 12(1), pp. 8-13. https://doi.org/10.1680/jgele.21.00097

Seed, H.B., Dunlop, P., & Lee, K.L., 1969. Effect of transient loading on the strength of sand. *Proceeding of the 7th International Conference on Soil Mechanics and Foundation Engineering*, pp. 239–247.

Sibille, L., 2006. *Modélisations discrètes de la rupture dans les milieux granulaires,* France: Doctoral Thesis Report. Sciences de l'ingénieur [physics]. Institut National Polytechnique de Grenoble – INPG

Svoboda, J., 2013. *Impact of strain rate on the shear strength and pore water pressure generation of clays and sands*, United States: Graduate Thesis Report. Department of Civil, Environmental and Architectural Engineering. University of Colorado Boulder.

Tan, X., Konietzky, H. & Fruhwirt, T., 2014. Laboratory observation and numerical simulation of permeability evolution during progressive failure of brittle rocks. *International Journal of Rock Mechanics and Mining Sciences.* https://doi.org/10.1016/j.ijrmms.2014.02.016

Tang, L., 2013. *Application of the discrete element method for concrete fracturing*. PhD Thesis, Swansea University, United Kingdom. https://doi.org/10.1057/978-1-349-96042-2_7971

Valera, R. R., Morales, I. P., Vanmaercke, S., Morfa, C. R., Cortés, L. A. & Casañas, H. D. G., 2015. Modified algorithm for generating high volume fraction sphere packings. *Computational Particle Mechanics*, 2(2), pp. 161–172. https://doi.org/10.1007/s40571-015-0045-8

Wen, R. et al., 2018. Grain Size Effect on the Mechanical Behavior of Cohesionless Coarse-Grained Soils with the Discrete Element Method. *Advances in Civil Engineering*. https://doi.org/10.1155/2018/4608930

Widuliński, Ł., Kozicki, J. & Tejchman, J., 2009. Numerical simulations of triaxial test with sand using DEM. *Archives of Hydroengineering and Environmental Mechanics*, 56(3–4), pp. 149–172.

Wu, M., Xiong, L. & Wang, J., 2021. DEM study on effect of particle roundness on biaxial shearing of sand. *Underground Space* (China), 6(6), pp. 678–694. https://doi.org/10.1016/j.undsp.2021.03.006

Yamamuro, J. A., Abrantes, A. E., & Lade, P. V., 2011. Effect of Strain Rate on the Stress-Strain Behavior of Sand. *Journal of Geotechnical and Geoenvironmental Engineering*, 137(12), pp. 1169–1178. https://doi.org/10.1061/(asce)gt.1943-5606.0000542

Yan, G., Yu, H. sui & McDowell, G., 2009. Simulation of granular material behaviour using DEM. *Procedia Earth and Planetary Science*, 1(1), pp. 598–605. https://doi.org/10.1016/j.proeps.2009.09.095

Yang, G. & Wang, X., 2012. Discrete element modeling for granular materials. *Electronic Journal of Geotechnical Engineering*, 17, pp. 2463–2474.

Zeghal, M., 2004. Discrete-element method investigation of the resilient behavior of granular materials. *Journal of Transportation Engineering,* 130(4), pp. 503–509. https://doi.org/10.1061/(ASCE)0733-947X(2004)130:4(503)

Zhao, S., Zhou, X. & Liu, W., 2015. Discrete element simulations of direct shear tests with particle angularity effect. *Granular Matter*, 17, pp. 793–806. https://doi.org/10.1007/s10035-015-0593-x

Zhu, H., Nicot, F. & Darve, F., 2016. Meso-structure evolution in a 2D granular material during biaxial loading. *Granular Matter,* 18(1), pp. 1–12. https://doi.org/10.1007/s10035-016-0608-2